Supporting Information

Rational design of hierarchically-structured $CuBi_2O_4$ composites by deliberate manipulation of the nucleation and growth kinetics of $CuBi_2O_4$ for environmental applications

Wen-Da Oh[a, b], Shun-Kuang Lua[a, c], Zhili Dong[a, c], Teik-Thye Lim[a, b*]

[a]Nanyang Environment and Water Research Institute (NEWRI), Interdisciplinary Graduate School (IGS), Nanyang Technological University, 1 Cleantech Loop, CleanTech One, Singapore 637141, Singapore.

[b]Division of Environmental and Water Resources Engineering, School of Civil and Environmental Engineering, Nanyang Technological University, 50 Nanyang Avenue, Singapore 639798, Singapore.

[c]School of Materials Science and Engineering, Nanyang Technological University, 50 Nanyang Avenue, Singapore 639798, Singapore.

Supplementary Info

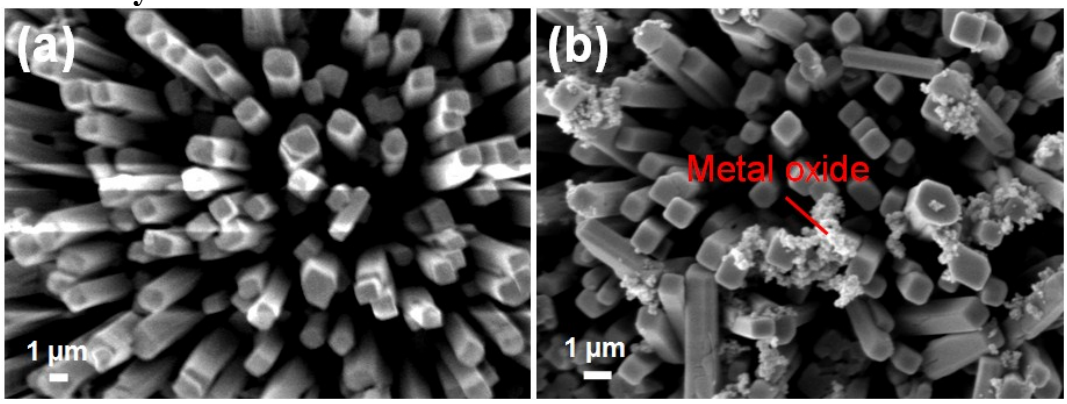

Fig. S1: The FESEM micrographs of (a) CuBi2O4 and (b) CuBi2O4 composite with auxiliary Co but without EG. The metal oxide could be visibly seen anchored on the surface of the CuBi2O4 nanorods.

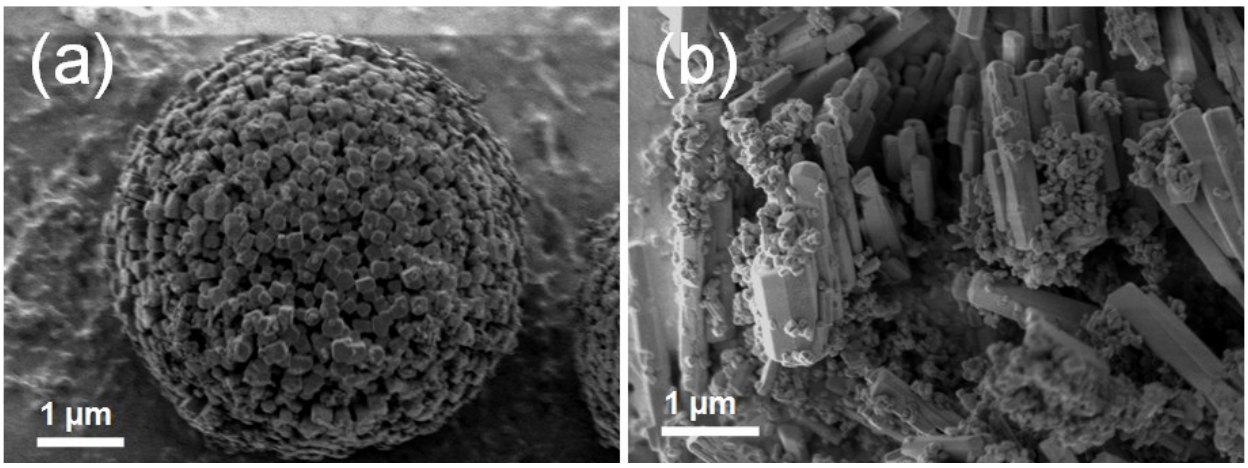

Fig. S2: The FESEM micrographs of $CuBi_2O_4$ composites synthesized (a) at 140°C and (b) with Cu^{2+} to $CuBi_2O_4$ ratio of 0.5:1. When Cu^{2+} to $CuBi_2O_4$ ratio is higher than 0.5:1, the resultant product is a mixture of nanorods and nanoparticles. When lower temperature was used, the $CuBi_2O_4$ prefer to grow and mature via isotropic Ostwald ripening due to relatively slower nucleation and growth kinetics. At higher temperature, $CuBi_2O_4$ prefer to grow and mature via anisotropic Ostwald ripening due to its relatively faster nucleation and growth kinetics.

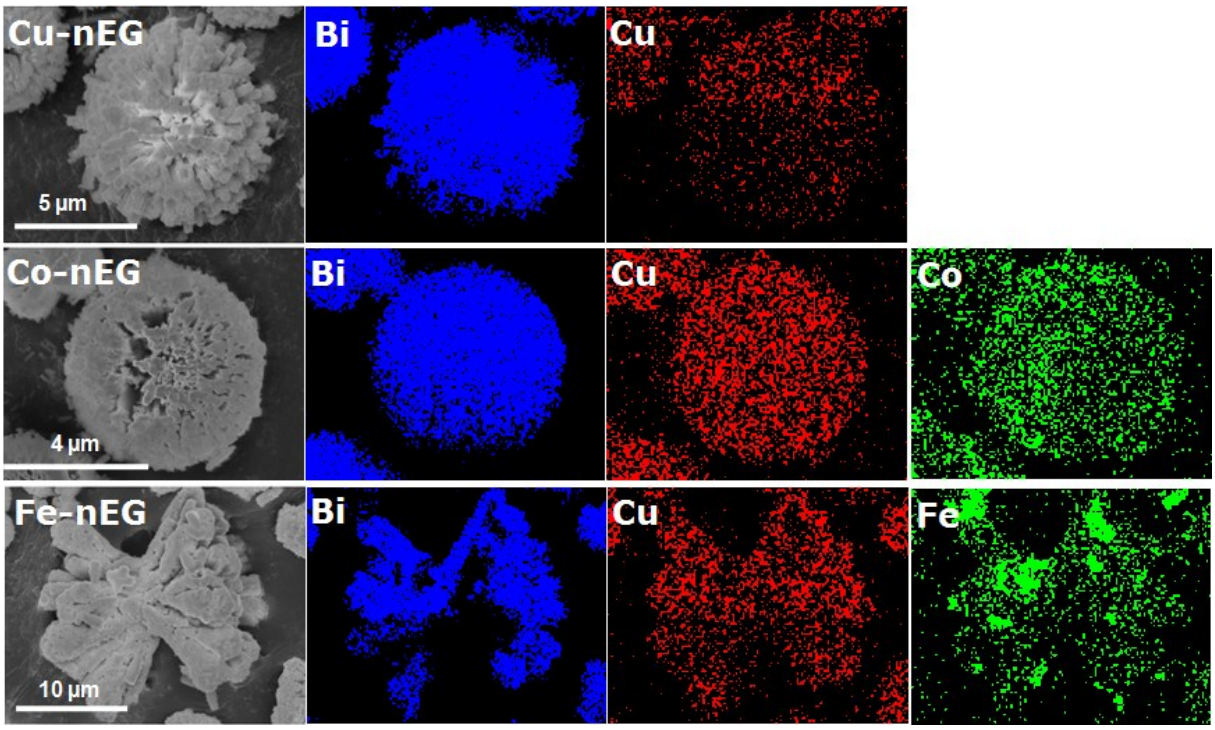

Fig. S3: Elemental mapping of CuO-CuB, CoO-CuB and FeO-CuB indicating relatively homogeneous distribution of the elements. This also provides clear evidence that the Co and Fe are present in the crystal system.

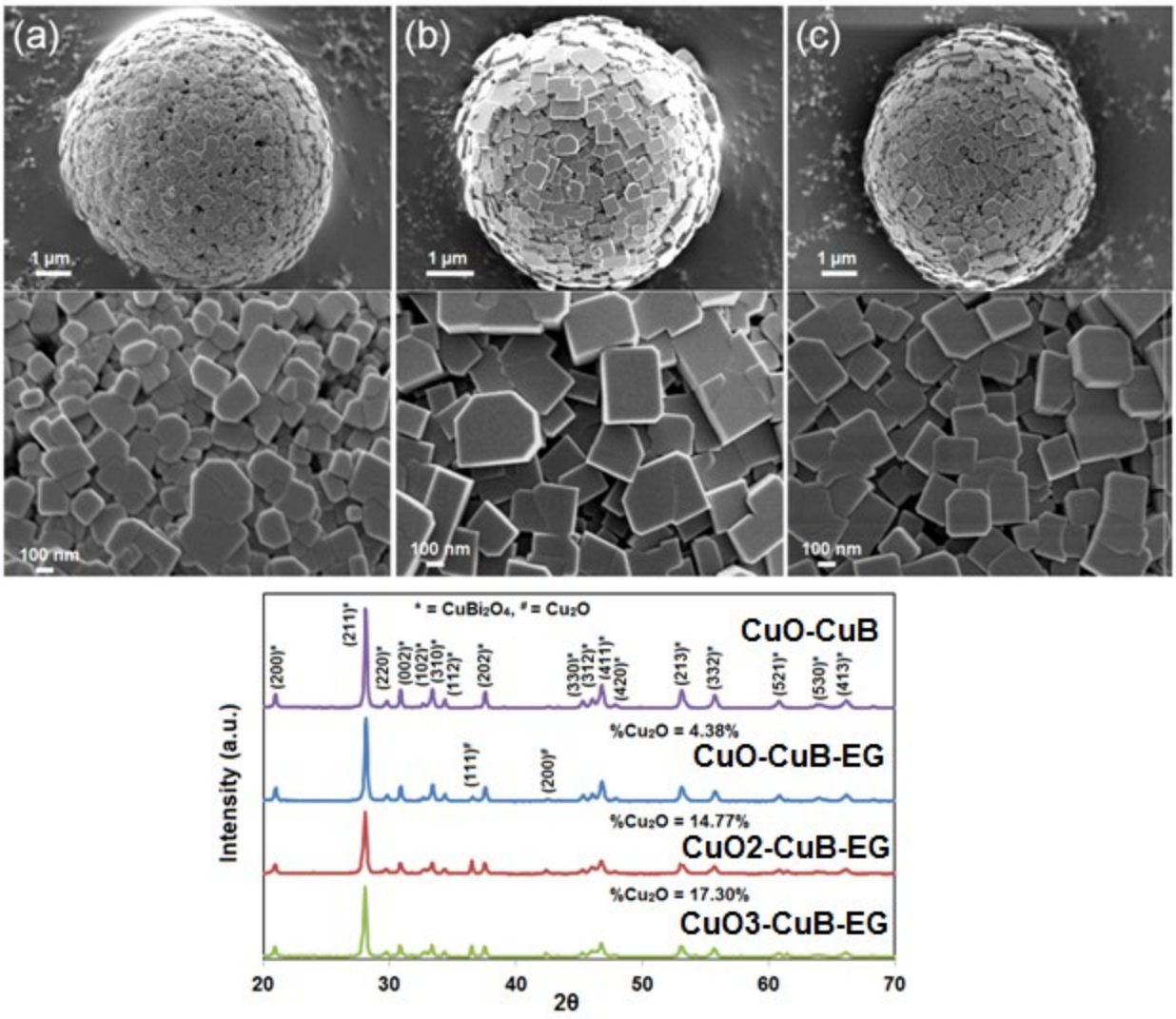

Fig. S4: The FESEM micrographs (single microsphere and surface) and % Cu_2O content determined using the rietveld refinement method. (a) CuO-CuB-EG, (b) CuO2-CuB-EG, and (c) CuO3-CuB-EG. The morphologies of the $CuBi_2O_4$ composites are similar. The close-up micrograph of the surface reveals Cu_2O cubic surface.

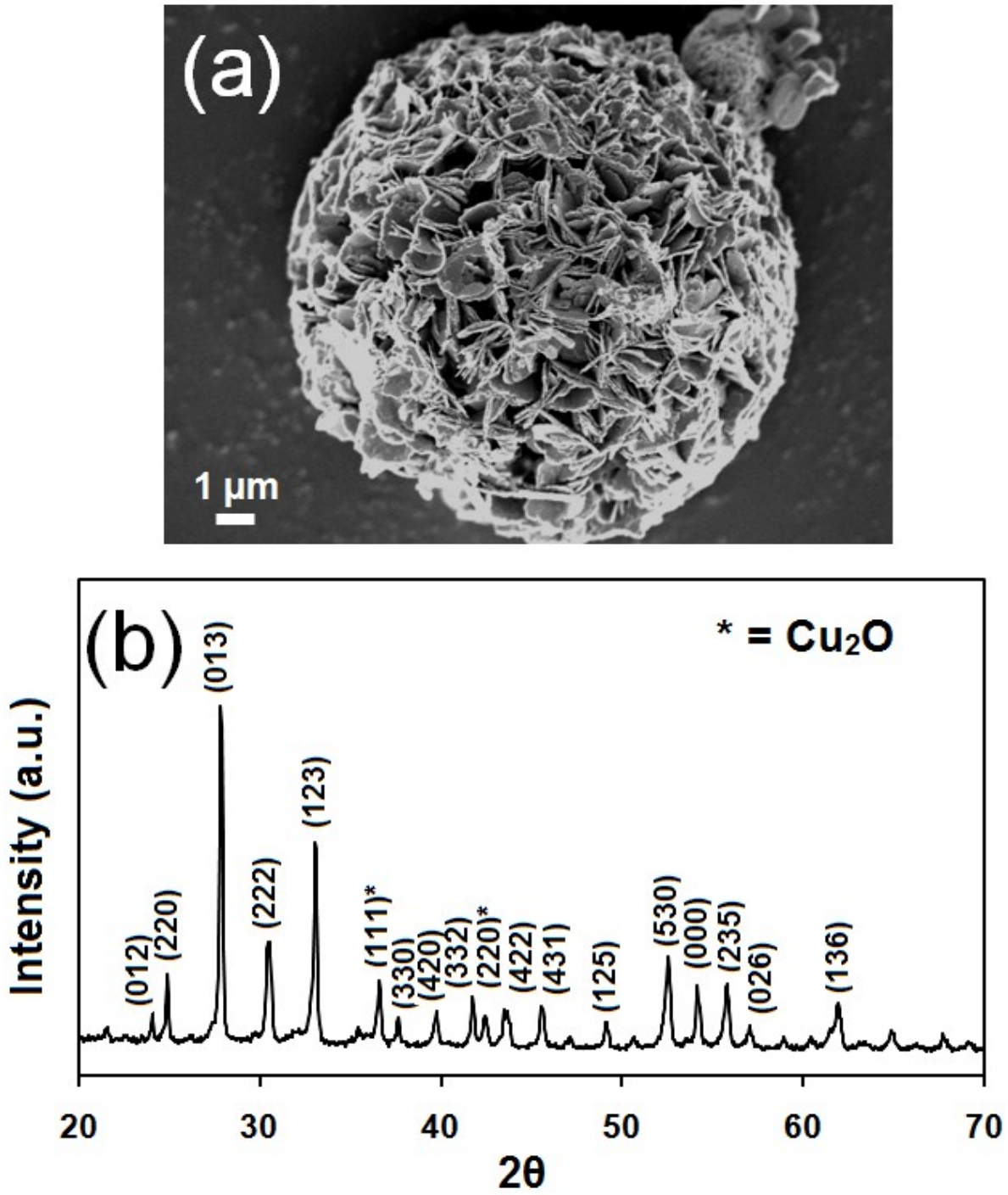

Fig. S5: The FESEM micrograph (a) and XRD pattern (b) of FeO-CuB-EG. The FESEM micrograph indicates that the FeO-CuB-EG has a pollen-grain-like morphology. The XRD pattern can be indexed to and Cu_2O.

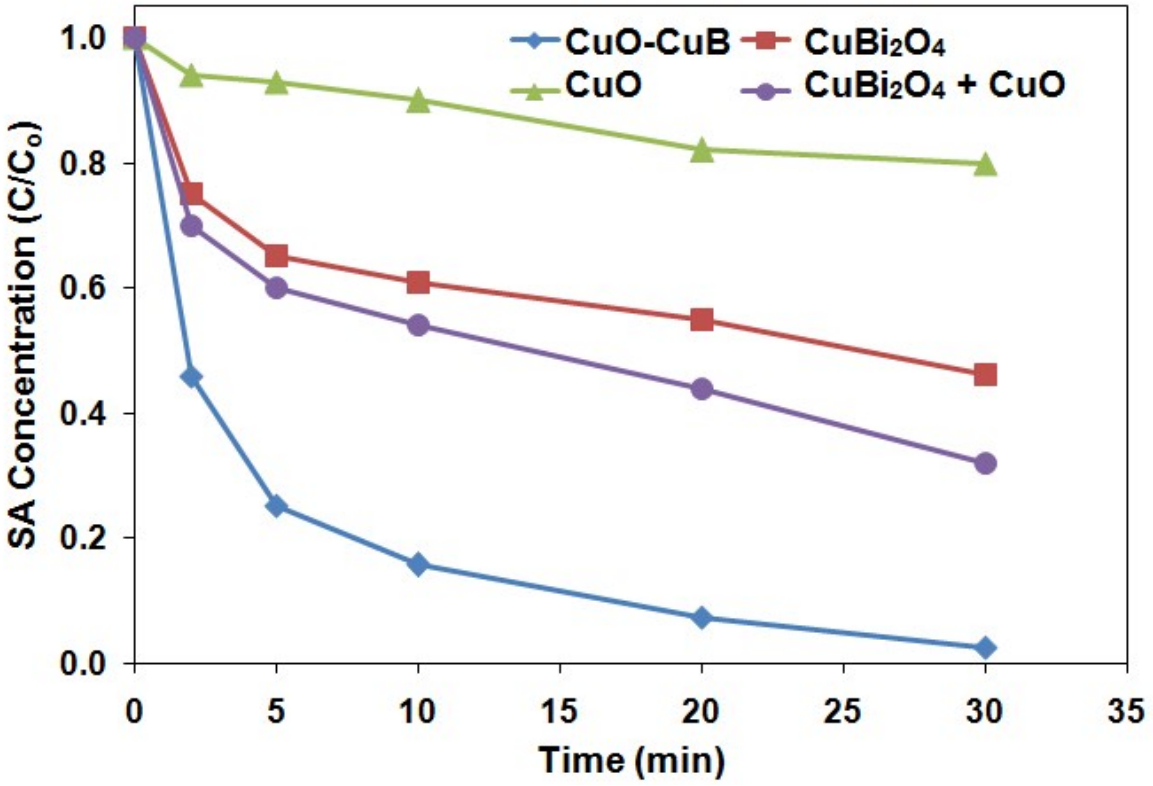

Fig. S6: The performance of CuO-CuB, $CuBi_2O_4$, CuO and CuO + $CuBi_2O_4$ for sulfanilamide removal via peroxymonosulfate activation. Initial conditions: [SA] = 2.5 mg L^{-1}, pH = 7.0, [CuO-CuB]&[$CuBi_2O_4$] = 0.4 g L^{-1} and CuO = 0.05 g L^{-1}. The performance of mechanically mixed $CuBi_2O_4$ (0.4 g L^{-1}) and CuO (0.05 g L^{-1}, with at least 5 times the loading of CuO-CuB) is lower than the CuO-CuB indicating synergistic effect exist between $CuBi_2O_4$ and metal oxide coupling.